Inorganic Chemistry
Article

Inorg. Chem. **2010**, *49*, 10617–10626 **10617**
DOI: 10.1021/ic1016142

Structural Comparison of Copper(I) and Copper(II) Complexes with Tris(2-pyridylmethyl)amine Ligand

William T. Eckenhoff and Tomislav Pintauer*

Department of Chemistry and Biochemistry, Duquesne University, 600 Forbes Avenue, 308 Mellon Hall, Pittsburgh, Pennsylvania 15282, United States

Received August 9, 2010

Copper(I) complexes with the tris(2-pyridylmethyl)amine (TPMA) ligand were synthesized and characterized to examine the effect of counteranions (Br^-, ClO_4^-, and BPh_4^-), as well as auxiliary ligands (CH_3CN, 4,4′-dipyridyl, and PPh_3) on the molecular structures in both solid state and solution. Partial dissociation of one of the pyridyl arms in TPMA was not observed when small auxiliary ligands such as CH_3CN or Br^- were coordinated to copper(I), but was found to occur with larger ones such as PPh_3 or 4,4′-dipyridyl. All complexes were found to adopt a distorted tetrahedral geometry, with the exception of $[Cu^I(TPMA)][BPh_4]$, which was found to be trigonal pyramidal because of stabilization via a long cuprophilic interaction with a bond length of 2.8323(12) Å. Copper(II) complexes with the general formula $[Cu^{II}(TPMA)X][Y]$ (X = Cl^-, Br^- and Y = ClO_4^-, BPh_4^-) were also synthesized to examine the effect of different counterions on the geometry of $[Cu^{II}(TPMA)X]^+$ cation, and were found to be isostructural with previously reported $[Cu^{II}(TPMA)X][X]$ (X = Cl^- or Br^-) complexes.

Introduction and Background

Tris(2-pyridylmethyl)amine (TPMA) is a widely used neutral tripodal nitrogen based ligand that has been complexed to a wide variety of transition metals. Currently, the Cambridge Crystallographic Database contains over 350 structures with metals spanning from group 1 to 13 of the periodic table, including many cases from the lanthanide and actinide series. TPMA is an excellent chelator that typically coordinates to a metal in a tetradentate fashion. However, in some cases, tridentate coordination achieved by pyridyl nitrogen arm dissociation has also been observed. Some representative structures of copper(I and II),[1,2] iron(II),[3] ruthenium(II),[4] and europium(III)[5] complexes with TPMA ligand are shown in Figure 1.

Over the past few years, TPMA has received considerable attention as a ligand of choice in copper complexes that mimic certain metalloenzymes of relevance to oxygen activation.[6−14] Also, on the other hand, it is complexes with copper that have been shown to be among the most active in atom transfer radical addition (ATRA)[15−17] and polymerization (ATRP).[18,19] Both processes originated from well-known Kharasch addition in which polyhalogenated compounds were added to alkenes via free-radical means.[20−22] Recent studies have also indicated that TPMA is a superior

*To whom correspondence should be addressed. E-mail: pintauert@duq.edu. Phone: 412-396-1626. Fax: 412-396-5683.

(1) Eckenhoff, W. T.; Garrity, S. T.; Pintauer, T. *Eur. J. Inorg. Chem.* **2008**, 563–571.
(2) Eckenhoff, W. T.; Pintauer, T. *Inorg. Chem.* **2007**, *46*, 5844–5846.
(3) Mandon, D.; Machkour, A.; Goetz, S.; Welter, R. *Inorg. Chem.* **2002**, *41*, 5364–5372.
(4) Bjernemose, J.; Hazell, A.; McKenzie, C. J.; Mahon, M. F.; Nielsena, L. P.; Raithby, P. R.; Simonsen, O.; Toftlund, H.; Wolny, J. A. *Polyhedron* **2003**, *22*, 875–885.
(5) Wietzke, R.; Mazzanti, M.; Latour, J. M.; Pecaut, J.; Cordier, P. Y.; Madic, C. *Inorg. Chem.* **1998**, *37*, 6690–6697.
(6) Baldwin, M. J.; Ross, P. K.; Pate, J. E.; Tyeklar, Z.; Karlin, K. D.; Solomon, E. I. *J. Am. Chem. Soc.* **1991**, *113*, 8671–8679.
(7) Fry, H. C.; Scaltrito, D. V.; Karlin, K. D.; Meyer, G. J. *J. Am. Chem. Soc.* **2003**, *125*, 11866–11871.
(8) Karlin, K. D.; Hayes, J. C.; Juen, S.; Hutchinson, J. P.; Zubieta, J. *Inorg. Chem.* **1982**, *21*, 4106–4108.
(9) Karlin, K. D.; Nanthakumar, A.; Fox, S.; Murthy, N. N.; Ravi, N.; Huynh, B. H.; Orosz, R. D.; Day, E. P. *J. Am. Chem. Soc.* **1994**, *116*, 4753–4763.
(10) Karlin, K. D.; Wei, N.; Jung, B.; Kaderli, S.; Niklaus, P.; Zuberbuhler, A. D. *J. Am. Chem. Soc.* **1993**, *115*, 9506–9514.
(11) Karlin, K. D.; Zubieta, J. *Copper Coordination Chemistry: Biochemical and Inorganic Perspectives*; Adenine Press: New York, 1983.
(12) Wei, N.; Lee, D.; Murthy, N. N.; Tyeklar, Z.; Karlin, K. D.; Kaderli, S.; Jung, B.; Zuberbuehler, A. D. *Inorg. Chem.* **1994**, *33*, 4625–4626.
(13) Wei, N.; Murthy, N. N.; Chen, Q.; Zubieta, J.; Karlin, K. D. *Inorg. Chem.* **1994**, *33*, 1953–1965.
(14) Tyeklar, Z.; Jacobson, R. R.; Wei, N.; Murthy, N. N.; Zubieta, J.; Karlin, K. D. *J. Am. Chem. Soc.* **1993**, *115*, 2677–2689.
(15) Clark, A. J. *Chem. Soc. Rev.* **2002**, *31*, 1–11.
(16) Eckenhoff, W. T.; Pintauer, T. *Catal. Rev. -Sci. Eng.* **2010**, *52*, 1–59.
(17) Pintauer, T. *Eur. J. Inorg. Chem.* **2010**, 2449–2460.
(18) Matyjaszewski, K.; Xia, J. *Chem. Rev.* **2001**, *101*, 2921–2990.
(19) Wang, J.-S.; Matyjaszewski, K. *J. Am. Chem. Soc.* **1995**, *117*, 5614–5615.
(20) Kharasch, M. S.; Engelmann, H.; Mayo, F. R. *J. Org. Chem.* **1937**, *2*, 288–302.
(21) Kharasch, M. S.; Jensen, E. V.; Urry, W. H. *Science* **1945**, *102*, 128–128.
(22) Kharasch, M. S.; Jensen, E. V.; Urry, W. H. *J. Am. Chem. Soc.* **1945**, *67*, 1626–1626.

Published on Web 10/12/2010

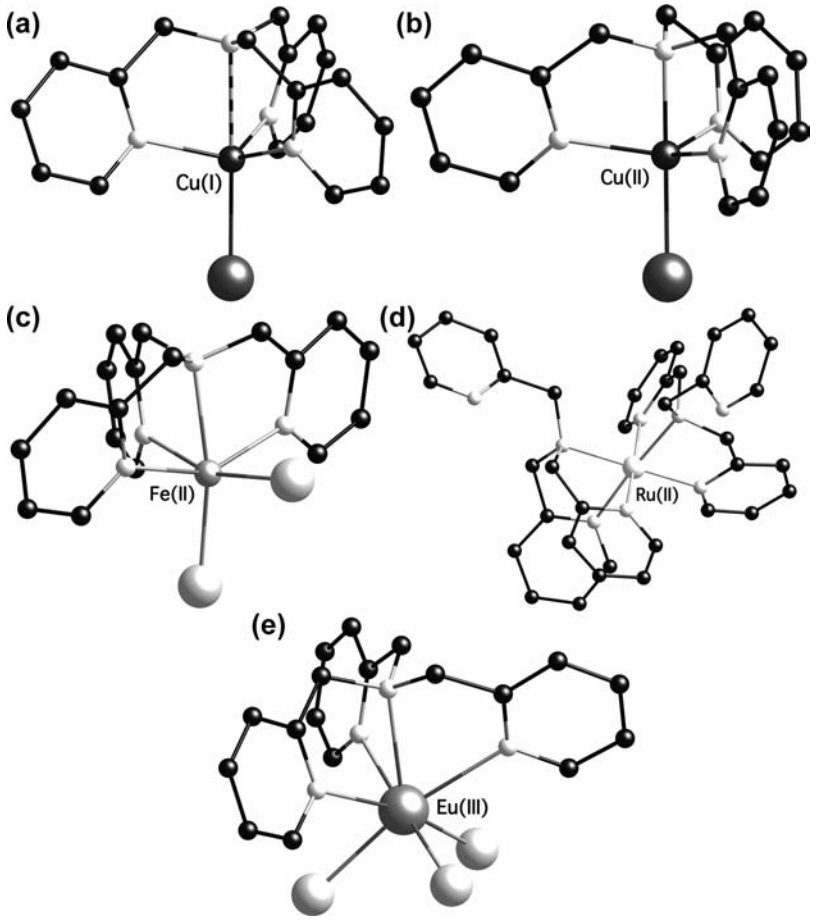

Figure 1. Examples of different transition metal complexes containing coordinated TPMA ligand; (a) Cu^{I}(TPMA)Br,[1] (b) [Cu^{II}(TPMA)Br][Br],[1] (c) $Fe^{II}(TPMA)Cl_2$,[2] (d) $[Ru^{II}(TPMA)_2][PF_6]_2$,[3] and (e) $Eu^{III}(TPMA)Cl_3$.[4]

complexing ligand in ATRA[1,2,16,17,23−32] and ATRP[26,33−36] that utilize reducing agents. The role of a reducing agent in both systems is to continuously regenerate the activator species (copper(I) complex) from the corresponding deactivator (copper(II) complex). The latter one accumulates in the system as a result of unavoidable and often diffusion controlled radical−radical termination reactions. This is schematically illustrated in Scheme 1 in the case of simple ATRA addition. ATRP is a mechanistically similar process with the exception that the structure of the starting alkyl halide and alkene (or monomer) are modified in such a way that multiple activation/deactivation cycles can occur. As a result, these synthetically useful reactions for the syntheses of small organic molecules and well-defined polymers can now be conducted using parts per million (ppm) amounts of copper.[26]

Scheme 1. Proposed Mechanism for Copper Catalyzed ATRA in the Presence of Radicals Generated by Thermal Decomposition of AIBN

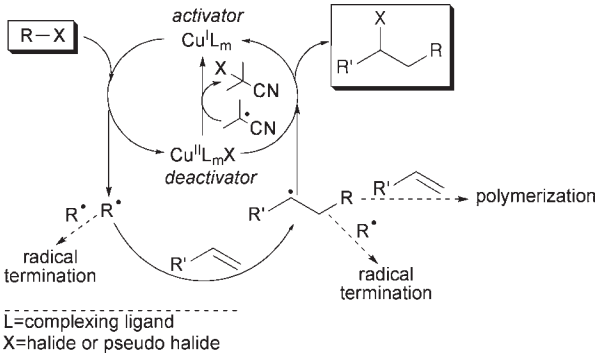

Despite a significant effort devoted to the use of copper(I) and copper(II) complexes with TPMA ligand in synthetic aspects of ATRA and ATRP, structural and mechanistic studies of this active catalytic system still need further

(23) Balili, M. N. C.; Pintauer, T. *Inorg. Chem.* **2009**, *48*, 9018–9026.
(24) Pintauer, T. *ACS Symp. Ser.* **2009**, *1023*, 63–84.
(25) Pintauer, T.; Eckenhoff, W. T.; Ricardo, C.; Balili, M. N. C.; Biernesser, A. B.; Noonan, S. J.; Taylor, M. J. W. *Chem.—Eur. J.* **2009**, *15*, 38–41.
(26) Pintauer, T.; Matyjaszewski, K. *Chem. Soc. Rev.* **2008**, *37*, 1087–1097.
(27) Pintauer, T.; Matyjaszewski, K. *Top. Organomet. Chem.* **2009**, *26*, 221–251.
(28) Ricardo, C.; Pintauer, T. *Chem. Commun.* **2009**, 3029–3031.
(29) Muñoz-Molina, J. M.; Belderraín, T. R.; Pérez, P. J. *Adv. Synth. Catal.* **2008**, *350*, 2365–2372.
(30) Muñoz-Molina, J. M.; Belderraín, T. R.; Pérez, P. J. *Inorg. Chem.* **2010**, *49*, 642–645.
(31) Muñoz-Molina, J. M.; Caballero, A.; Díaz-Requejo, M. M.; Trofimenko, S.; Belderraín, T. R.; Pérez, P. J. *Inorg. Chem.* **2007**, *46*, 7725–7730.
(32) Balili, M. N. C.; Pintauer, T. *Inorg. Chem.* **2010**, *49*, 5642–5649.
(33) Jakubowski, W.; Matyjaszewski, K. *Macromolecules* **2005**, *38*, 4139–4146.
(34) Jakubowski, W.; Matyjaszewski, K. *Angew. Chem., Int. Ed.* **2006**, *45*, 4482–4486.
(35) Jakubowski, W.; Min, K.; Matyjaszewski, K. *Macromolecules* **2006**, *39*, 39–45.
(36) Matyjaszewski, K.; Jakubowski, W.; Min, K.; Tang, W.; Huang, J.; Braunecker, W. A.; Tsarevsky, N. V. *Proc. Natl. Acad. Sci. U.S.A.* **2006**, *103*, 15309–15314.

Scheme 2. Proposed Equilibria for Cu^{I}(TPMA)Br Involving Bromide Anion and Pyridine Nitrogen Association/Dissociation

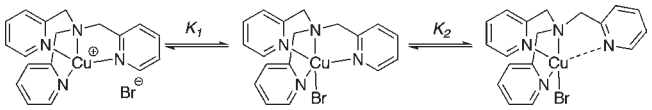

investigation. Recently, the molecular structures of Cu^{I}(TPMA)Cl and Cu^{I}(TPMA)Br were elucidated and surprisingly, taking into account the tetradentate nature of TPMA ligand, the copper(I) centers were found to contain coordinated halide anions (Figure 1a).[1,2] While these complexes can be seen as pseudo-pentacoordinated, they were formally described as distorted tetrahedral because of the elongated Cu−N axial bond. It was further hypothesized that the high activity of Cu^{I}(TPMA)X and the corresponding $[Cu^{II}(TPMA)X][X]$ (X = Br^{-} or Cl^{-}) complexes in ATRA can be explained by the fact that minimum entropic rearrangement was required upon oxidation and reduction. However, the presence of coordinated halide anions raised further questions regarding the catalytic mechanism of ATRA, which was conventionally described as an inner sphere electron transfer (ISET).[18,37−40] The outer sphere electron transfer (OSET) mechanism,[18,37,38,40] while theoretically feasible, was recently probed by extensive ab initio calculations, which concluded that OSET was approximately 12 orders of magnitude slower than the ISET, clearly making this an unlikely scenario. Therefore, the ISET process for copper(I) halide complexes with TPMA ligand would require an open coordination site, and is most likely preceded by either dissociation of the halide anion or one arm of TPMA, as indicated in Scheme 2.

Dynamic behavior of Cu^{I}(TPMA)X (X = Br^{-} and Cl^{-}) was further probed by ^{1}H NMR spectroscopy, which confirmed that the most probable structure in solution was in fact a monomer with chemically equivalent pyridyl arms.[1,41] Coordination of a solvent molecule, such as acetone, could theoretically also produce a symmetrical monomeric structure, but no evidence was found to suggest this. Hence, bromide anion was assumed to be the coordinating auxiliary ligand. Isolation of a dimeric complex, $[Cu^{I}(TPMA)]_2[ClO_4]_2$,[42] was achieved in the absence of a coordinating solvent or ligand, and the variable temperature ^{1}H NMR showed, as expected, all three pyridyl arms as chemically distinct. This also suggested that the bromide anion was bound to copper in solution in the case of Cu^{I}(TPMA)Br, thus preventing dimer formation. Similar conclusions were also drawn for Cu^{I}(TPMA)Cl complex.

To further investigate the role of the anion, copper(I and II) complexes were synthesized with a variety of counterions such as perchlorate (ClO_4^{-}), hexafluorophosphate (PF_6^{-}), and tetraphenylborate (BPh_4^{-}). However, complexes with these "non-coordinating" anions were found to be less reducing by approximately 300 mV, when compared to their halide analogues.[1] These results also indicated that such complexes should be substantially less active in ATRA systems based on the linear correlation of $E_{1/2}$ values with the equilibrium constant for atom transfer (K_{ATRA}).[18,27,43−46] Clearly, the counterion in the copper(I) state, which was previously thought to be merely a spectator ion, plays an important role in the reaction mechanism.

In this article, copper(I and II) complexes with TPMA ligand were synthesized, and counterion and coordinating ligand effects on the catalyst structure in the solid state and solution examined.

Experimental Section

General Procedures. All chemicals were purchased from commercial sources and used as received. Tris(2-pyridylmethyl)amine (TPMA)[47] and $[Cu^{I}(CH_3CN)_4][ClO_4]$[48] were synthesized according to literature procedures. ***Caution!*** *Although we have experienced no problems, perchlorate metal salts are potentially explosive and should be handled with care*. All manipulations involving copper(I) complexes were performed under argon atmosphere in the drybox (< 1.0 ppm O_2 and < 0.5 ppm H_2O), or using standard Schlenk line techniques. Solvents (pentane, acetonitrile, acetone, and diethyl ether) were degassed and deoxygenated using an Innovative Technology solvent purifier. Methanol was vacuum distilled and deoxygenated by bubbling argon for 30 min prior to use. Synthesis of copper(II) complexes were performed in ambient conditions and solvents were used as received. ^{1}H NMR spectra were obtained using Bruker Avance 400 and 500 MHz spectrometers and chemical shifts are given in ppm relative to residual solvent peaks ($CDCl_3$ δ7.26 ppm; $(CD_3)_2CO$ δ2.05 ppm; CD_3CN δ1.96 ppm). ^{31}P NMR was referenced externally with 85% H_3PO_4 in D_2O at δ0. iNMR software and Kaleidagraph were used to generate images of NMR spectra. Temperature calibrations were performed using a pure methanol sample. IR spectra were recorded in the solid state using a Nicolet Smart Orbit 380 FT-IR spectrometer (Thermo Electron Corporation). Elemental analyses for C, H, and N were obtained from Midwest Microlabs, LLC.

X-ray Crystal Structure Determination. The X-ray intensity data were collected at 150 K using graphite-monochromated Mo−K radiation (0.71073 Å) with a Bruker Smart Apex II CCD diffractometer. Data reduction included absorption corrections by the multiscan method using SADABS.[49] Structures were solved by direct methods and refined by full matrix least-squares using SHELXTL 6.1 bundled software package.[50] The H-atoms were positioned geometrically (aromatic C−H 0.93, methylene C−H 0.97, and methyl C−H 0.96) and treated as riding atoms during subsequent refinement, with $U_{iso}(H) = 1.2U_{eq}(C)$ or $1.5U_{eq}$(methyl C). The methyl groups were allowed to rotate about their local 3-fold axes. ORTEP-3 for windows[51] and Crystal Maker 7.2 were used to generate molecular graphics.

$[Cu^{I}(TPMA)(CH_3CN)][BPh_4]$ (1). TPMA (89.0 mg, 0.306 mmol) was dissolved in 2 mL of methanol followed by addition of $[Cu^{I}(CH_3CN)_4][ClO_4]$ (100 mg, 0.306 mmol), resulting in a yellow

(37) Kochi, J. K. *Free Radicals*; John Wiley & Sons: New York, 1973; Vol. *1*.
(38) Lin, C. Y.; Coote, M. L.; Gennaro, A.; Matyjaszewski, K. *J. Am. Chem. Soc*. **2008**, *130*, 12762–12774.
(39) Matyjaszewski, K. *Macromolecules* **1998**, *31*, 4710–4717.
(40) Tsarevsky, N. V.; Braunecker, W. A.; Matyjaszewski, K. *J. Organomet. Chem*. **2007**, *692*, 3212–3222.
(41) Hsu, S. C.; Chien, S. S.; Chen, H. H.; Chiang, M. Y. *Chin. Chem. Soc*. **2007**, *54*, 685–692.
(42) Eckenhoff, W. T.; Manor, B. C.; Pintauer, T. *Polym. Prepr*. (*Am. Chem. Soc., Div. Polym. Chem.*) **2008**, *49*(2), 213–214.
(43) Matyjaszewski, K.; Gobelt, B.; Paik, H.-j.; Horwitz, C. P. *Macromolecules* **2001**, *34*, 430–440.
(44) Qiu, J.; Matyjaszewski, K.; Thounin, L.; Amatore, C. *Macromol. Chem. Phys*. **2000**, *201*, 1625–1631.
(45) Tang, W.; Kwak, Y.; Braunecker, W.; Tsarevsky, N. V.; Coote, M. L.; Matyjaszewski, K. *J. Am. Chem. Soc*. **2008**, *130*, 10702–10713.
(46) Tang, W.; Tsarevsky, N. V.; Matyjaszewski, K. *J. Am. Chem. Soc*. **2006**, *128*, 1598–1604.
(47) Britovsek, G.; England, J.; White, A. *Inorg. Chem*. **2005**, *44*, 8125–8134.
(48) Munakata, M.; Kitagawa, S.; Asahara, A.; Masuda, H. *Bull. Chem. Soc. Jpn*. **1987**, *60*, 1927–1929.
(49) Sheldrick, G. M. *SADABS*, Version 2.03; University of Göttingen: Göttingen, Germany, 2002.
(50) Sheldrick, G. M. *SHELXTL,Crystallographic Computing System*, 6.1; Bruker Analytical X-Ray System: Madison, WI, 2000.
(51) Faruggia, L. J. *J. Appl. Crystallogr*. **1997**, *30*(5, Pt. 1), 565.

solution. $NaBPh_4$ (105 mg, 0.306 mmol) was then added to the reaction mixture, which resulted in immediate precipitation of a yellow powder. The crude product was filtered, thoroughly washed with methanol, and redissolved in acetonitrile, resulting in a red solution. [Cu^I(TPMA)(CH_3CN)][BPh_4] was precipitated as an orange powder by slow addition of diethyl ether (yield = 137 mg, 62%). X-ray quality crystals were obtained by crystallization in acetonitrile via slow diffusion of diethyl ether. ^{1}H NMR ((CD_3)$_2$CO, 400 MHz, 180 K): δ9.17 (d, J = 4.7 Hz, 3H), δ7.77 (td, J = 7.6, 1.5 Hz, 3H), δ7.39 (d, J = 7.8 Hz, 4H), δ7.30 (m, 4H), δ7.10 (m, 3H), δ6.92 (t, J = 7.3 Hz, 4H), δ6.76 (t, J = 7.2 Hz, 2H), δ4.03 (s, 6H), δ 3.54 (s, 3H). FT-IR (solid): ν (cm^{-1}) = 3058 (m), 1599 (m), 1573 (w), 1475 (m), 1434 (m), 1367 (w), 1269 (w), 1153 (w), 1051 (w), 974 (w), 841 (w), 764 (m), 746 (m), 733 (s), 704 (s), 611 (s). Anal. Calcd. for $C_{44}H_{41}N_5CuB$ (714.17): C, 74.00; H, 5.79; N, 9.81. Found C, 73.89; H, 6.01; N, 9.67.

[Cu^I(TPMA)][BPh_4] (2). TPMA (89.0 mg, 0.306 mmol) was dissolved in 2 mL of methanol followed by addition of [Cu^I-(CH_3CN)$_4$][ClO_4] (100 mg, 0.306 mmol), resulting in a yellow solution. $NaBPh_4$ (105 mg, 0.306 mmol) was then added to the reaction mixture which resulted in immediate precipitation of a yellow powder. The crude product was washed thoroughly with methanol to yield 156 mg (76%) of [Cu^I(TPMA)][BPh_4]. Crystals suitable for X-ray diffraction were obtained in acetone via slow diffusion of diethyl ether. ^{1}H NMR ((CD_3)$_2$CO, 400 MHz, 298 K): δ8.67 (s, 3H), δ7.82 (td, J = 7.7, 1.3 Hz, 3H), δ7.43 (d, J = 7.8 Hz, 3H), δ7.38−7.33 (m, 12H), δ6.92 (t, J = 7.4 Hz, 7H), δ6.77 (t, J = 7.2 Hz, 4H), δ4.15 (bs, 6H). FT-IR (solid): ν(cm^{-1}) = 3053(w), 2982(w), 1601(m), 1475(m), 1427(m), 1269(w), 1134(w), 1101(w), 762(m), 733(s), 702(s), 611(m), 501(w). Anal. Calcd. for $C_{42}H_{38}N_4CuB$ (673.14): C, 74.94; H, 5.69; N, 8.32. Found: C, 74.63; H, 5.66; N, 8.13.

[(Cu^I(TPMA))$_2$-μ-Br][BPh_4] (3). Cu^I(TPMA)Br (100 mg, 0.231 mmol), previously synthesized according to published procedures,[1] was dissolved in 5 mL of methanol followed by addition of half an equivalent of $NaBPh_4$ (39.4 mg, 0.115 mmol). Although the precipitation of yellow powder occurred immediately, it quickly dissolved back into the reaction mixture, resulting in the formation of an orange solution. Upon slow addition of diethyl ether or tetrahydrofuran (THF), [(Cu^I(TPMA))$_2$-μ-Br][BPh_4] precipitated as a red-orange powder (yield = 81.0 mg, 32%). X-ray quality crystals were obtained in acetone via slow diffusion of diethyl ether. ^{1}H NMR ((CD_3)$_2$CO, 400 MHz, 180 K): δ9.17 (d, J = 3.8 Hz, 6H), δ7.78 (t, J = 7.4 Hz, 6H), δ7.40 (d, J = 7.7 Hz, 6H), δ7.31 (m, 8H), δ 7.08 (m, 6H), δ6.92 (m, 8H), δ6.76 (m, 4H), δ4.03 (bs, 12H). FT-IR (solid): ν (cm^{-1}) = 3051(w), 2982(w), 2885(w), 2843(w), 1597(m), 1566(w), 1473(m), 1427(m), 1365(w), 1315(w), 1150(m), 1049(m), 975(w), 894(w), 758(s), 725(s), 706(s), 613(m), 501(m). Anal. Calcd. for $C_{60}H_{56}N_8Cu_2BrB$ (1106.95): C, 65.10; H, 5.10; N, 10.12. Found: C, 65.00; H, 5.19; N, 10.15.

[Cu^I(TPMA)]$_2$[ClO_4]$_2$*CH_3OH (4). [Cu^I(CH_3CN)$_4$][ClO_4] (50.0 mg, 0.153 mmol) and TPMA (44.4 mg, 0.153 mmol) were dissolved in 1.0 mL of methanol. The vial was then sealed and placed in the freezer for 2 days, after which yellow crystals suitable for X-ray analysis were obtained (yield = 48.0 mg, 35%). ^{1}H NMR ((CD_3)$_2$CO, 400 MHz, 185 K): δ8.54 (d, J = 4.4 Hz, 2H), δ8.26 (d, J = 4.4 Hz, 2H), δ8.06 (m, 4 H), δ7.81 (t, J = 7.2, 2H), δ7.73 (d, J = 5.2, 2H), δ7.54 (pt, J = 7.6, 4H), δ7.24 (pt, J = 2.6, 4H), δ7.11 (t, J = 6.0, 2H), δ6.95 (t, J = 6.0, 2H), δ4.82 (d, J = 11.6, 2H), δ4.69 (d, J = 14.4, 2H), δ4.57 (m, J = 14.0, 4H), δ4.17 (dd, J = 23.1, 16.2 Hz, 4H). FT-IR (solid): ν (cm^{-1}) = 3068 (w), 2881 (w), 2359 (w), 2159 (w), 1600 (m), 1547 (w), 1477 (m), 1435 (m), 1082 (s), 724 (m), 620 (m). Anal. Calcd. for $C_{36}H_{36}N_8Cu_2Cl_2O_8$ (906.72): C, 47.69; H, 4.00; N, 12.36. Found: C, 47.72; H, 4.29; N, 12.27.

[(Cu^I(TPMA))$_2$(4,4′-dipy)][BPh_4]$_2$ (5) and [Cu^I(TPMA)(4,4′-dipy)][BPh_4] (6). [Cu^I(TPMA)][BPh_4] (135 mg, 0.201 mmol) was dissolved in 10.0 mL of acetone followed by addition of 5 equiv of 4,4′-dipyridyl (156 mg, 1.00 mmol), which resulted in a dark red solution. Crystals of X-ray quality were obtained in acetone by slow diffusion of diethyl ether, and contained both [(Cu^I(TPMA))$_2$(4,4′-dipy)][BPh_4]$_2$ and [Cu^I(TPMA)(4,4′-dipy)][BPh_4] in the asymmetric unit.

[Cu^I(TPMA)(PPh_3)][BPh_4] (7). [Cu^I(TPMA)][BPh_4] (100 mg, 0.149 mmol) was dissolved in 3.0 mL of acetone, and PPh_3 (39.0 mg, 0.149 mmol) was added, which resulted in a light yellow solution. Crystallization occurred immediately, producing colorless crystals suitable for X-ray analysis (yield = 109 mg, 78%). ^{1}H NMR ((CD_3)$_2$CO, 400 MHz, 180 K): δ8.46 (d, J = 4.4 Hz, 3H), δ7.88 (td, J = 7.7, 1.6 Hz, 3H), δ7.54 (m, 10H), δ7.39 (m, 11H), δ7.30 (m, 8H), δ6.92 (t, J = 7.4 Hz, 8H), δ6.76 (t, J = 7.1 Hz, 4H), δ4.17 (bs, 6H). ^{31}P NMR ((CD_3)$_2$CO, 162 MHz, 220 K): δ 2.88. FT-IR (solid): ν (cm^{-1}) = 3051(w), 2997(w), 1581(w), 1477(m), 1434(m), 1265(w), 1095(w), 841(w), 733(s), 702(s), 609(m), 498(m). Anal. Calcd. for $C_{60}H_{53}BCuN_4P$ (935.42): C, 77.04; H, 5.71; N, 5.99. Found: C, 76.69; H, 5.70; N, 5.92.

[Cu^{II}(TPMA)Cl][ClO_4] (8). [Cu^{II}(TPMA)Cl][Cl] (50.0 mg, 0.118 mmol), synthesized by previously reported methods,[2] was dissolved in 5.0 mL of methylene chloride and $NaClO_4$ (14.4 mg, 0.118 mmol) added. After stirring overnight, NaCl was filtered from the solution and blue powder precipitated by slow addition of pentane. [Cu^{II}(TPMA)Cl][ClO_4] was collected by filtration and dried under vacuum (yield = 34.0 mg, 59%). Crystals suitable for X-ray analysis were obtained in acetonitrile by slow diffusion of diethyl ether. FT-IR (solid): ν (cm^{-1}) = 3066(w), 2935(w), 1608(m), 1574(w), 1477(m), 1435(m), 1308(w), 1265(w), 1076(s), 764(m), 621(s). Anal. Calcd. for $C_{18}H_{18}N_4CuCl_2O_4$ (488.81): C, 44.23; H, 3.71; N, 11.46. Found: C, 44.25; H, 3.76; N, 11.41.

[Cu^{II}(TPMA)Cl][BPh_4]*CH_3CN (9). [Cu^{II}(TPMA)Cl][Cl] (50.0 mg, 0.118 mmol), synthesized by previously reported methods,[2] was dissolved in 3.0 mL of methanol followed by the addition of $NaBPh_4$ (40.3 mg, 0.118 mmol). Precipitation of a green powder occurred immediately. The crude product was washed with methanol, collected by filtration, and dried under vacuum to yield 64.5 mg (77%) of [Cu^{II}(TPMA)Cl][BPh_4]. Crystals of [Cu^{II}(TPMA)Cl][BPh_4]*CH_3CN suitable for X-ray analysis were obtained in acetonitrile by slow diffusion of diethyl ether. FT-IR (solid): ν (cm^{-1}) = 3054(w), 2989(w), 2931(w), 1605(m), 1574(w), 1477(m), 1427(m), 1261(m), 1022(m), 737(s), 710(s), 613(m), 505(w). Anal. Calcd. for $C_{44}H_{41}N_5CuClB$ (749.64): C, 70.50; H, 5.51; N, 9.34. Found: C, 70.35; H, 5.63; N, 9.36.

[Cu^{II}(TPMA)Br][ClO_4] (10). [Cu^{II}(TPMA)Br][Br] (100 mg, 0.195 mmol), synthesized by previously reported methods,[1] was dissolved in 5.0 mL of methylene chloride and $NaClO_4$ (23.9 mg, 0.195 mmol) added. After stirring overnight, NaBr was removed from the reaction mixture by filtration and blue powder precipitated by slow addition of pentane. [Cu^{II}(TPMA)Br][ClO_4] was collected by filtration and dried under vacuum (yield = 50.0 mg, 47%). Crystals suitable for X-ray analysis were obtained in acetonitrile by slow diffusion of diethyl ether. FT-IR (solid) ν (cm^{-1}) = 3066(w), 1608(w), 1477(m), 1308(m), 1265(w), 1080(s), 652(m), 621(s), 505(m). Anal. Calcd. for $C_{18}H_{18}N_4CuClBrO_4$ (533.26): C, 40.54; H, 3.40; N, 10.51. Found: C, 40.54; H, 3.39; N, 10.45.

[Cu^{II}(TPMA)Br][BPh_4]*CH_3CN (11). [Cu^{II}(TPMA)Br][Br] (100 mg, 0.193 mmol), synthesized by previously reported methods,[1] was dissolved in 3.0 mL of methanol and $NaBPh_4$ (66.0 mg, 0.193 mmol) added. Green powder which precipitated immediately was washed with methanol, collected by filtration, and dried under vacuum to yield 95.0 mg (65%) of [Cu^{II}(TPMA)Br][BPh_4]. Crystals of [Cu^{II}(TPMA)Br][BPh_4]*CH_3CN suitable for X-ray analysis were obtained in acetonitrile by slow diffusion of diethyl ether. FT-IR (solid): ν (cm^{-1}) = 3055(w), 2997(w), 2931(w), 1605(m), 1574(m), 1477(m), 1427 (m), 1261(m), 1022(m), 733(s), 706(s), 613(m), 505(m). Anal. Calcd. for $C_{44}H_{41}N_5CuBBr$ (794.09): C, 66.55; H, 5.20; N, 8.82. Found: C, 66.47; H, 5.16; N, 8.79.

Results and Discussion

Solid State Structural Studies of Copper(I) Complexes. Following the structural elucidation of Cu^I(TPMA)Cl

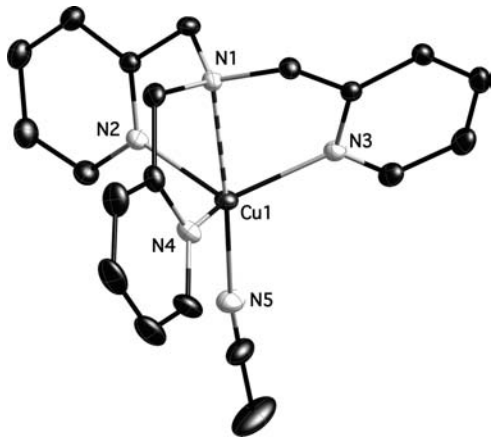

Figure 2. Molecular structure of $[Cu^{I}(TPMA)CH_3CN][BPh_4]$ (**1**) at 150 K, shown with 50% probability displacement ellipsoids. H-atoms and counteranion have been omitted for clarity. Selected distances [Å] and angles [deg]: Cu1−N1 2.4109(10), Cu1−N2 2.1031(10), Cu1−N3 2.1114(11), Cu−N4 2.0624(10), Cu1−N5 1.9914(11), N1−Cu1−N2 74.47(4), N1−Cu1−N3 74.04(4), N1−Cu1−N4 76.08(3), N1−Cu1−N5 175.94(4), N2−Cu1−N3 109.44(4), N2−Cu1−N4 115.97(4), N2−Cu1−N5 104.02(5), N3−Cu1−N4 114.92(4), N3−Cu1−N5 103.19(5), N4−Cu1−N5 107.90(5).

and Cu^{I}(TPMA)Br, it was immediately observed that these complexes were pseudo-pentacoordinated in the solid state because of the coordination of halide anions to the copper(I) centers.[1,2] These results were not expected, particularly taking into account the strong preference for copper(I) complexes to adopt tetrahedral geometry and the tetradentate nature of TPMA ligand. However, after careful examination, it was observed that the copper-amine ($Cu-N_{am}$) bond length in both complexes was slightly elongated at approximately 2.4 Å, when compared to a typical Cu−N bond (2.0−2.1 Å). Additionally, the copper atom in each complex was positioned below the least-squares-plane (LSP) derived from three pyridyl nitrogen atoms by approximately 0.53 Å. Therefore, copper(I) halide complexes containing TPMA ligand can be best described as formally being distorted tetrahedral in geometry, as a result of this elongation.

It was initially hypothesized that the elongation was the result of the large halide anion coordinated to copper on the opposing axial site.[42] To test this, $[Cu^{I}(TPMA)CH_3CN][BPh_4]$ (**1**) was synthesized via salt metathesis of Cu^{I}(TPMA)Br with $NaBPh_4$ in acetonitrile (Figure 2). The axial $Cu1-N_{am}$ bond in **1** was found to be elongated with a bond length of 2.4109(10) Å, and the $Cu-N_{py}$ bonds ranged from 2.0624(10) to 2.1114(11) Å. These results are in good agreement with previously characterized Cu^{I}(TPMA)Cl and Cu^{I}(TPMA)Br complexes.[1,2] Also, on the other hand, the copper(I) center was positioned below the LSP derived from N2, N3, and N4 toward the acetonitrile by 0.545(6) Å. The same distances in Cu^{I}(TPMA)Cl and Cu^{I}(TPMA)Br were found to be 0.534(6) Å and 0.538(6) Å, respectively.[1,2] The discussed Cu−N bond lengths in **1** also compare very well with previously reported complexes of similar structure (Table 1).[12−14,52,53]

In complex **1**, the Cu1−N5 bond was the shortest bond in the coordination sphere with a bond distance of 1.9914(11) Å. The $N_{am}-Cu1-N_{py}$ angles were found to be acute as a result, ranging from 74.04(4)° to 76.08(3)°. The larger bond angles between the copper atom and pyridine/acetonitrile nitrogen atoms ($N_{py}-Cu-N_{py}$ and $N_{py}-Cu-N5$) were between 103.19(4)° and 115.97(4)°. The coordinated acetonitrile molecule was nearly linear (C−N−C bond angle = 178.68(6)°) and bent by 11.79(6)° from the Cu−N5 bond toward the N4 pyridine ring. With this exception, $[Cu^{I}(TPMA)(CH_3CN)]^{+}$ cation had near perfect (non-crystallographic) C_3 symmetry. In the unit cell, the absence of available heteroatoms resulted in only weak C---H−C interactions between TPMA ligands, which ranged between 2.823(6) and 2.898(6) Å (see Supporting Information).

Because of the axial elongation observed in **1**, the nature of the auxiliary ligand can therefore be ruled out as causing $Cu-N_{am}$ elongation that was previously observed in copper(I) halide complexes with TPMA ligand. Although the preferred geometry for copper(I) is tetrahedral, the rigid structure of TPMA restricts such an arrangement. The elongation of the $Cu-N_{am}$ bond and the long distance of copper to the LSP derived from nitrogen atoms in pyridine rings is likely the result of a distorted-tetrahedral geometry comprising of three nitrogen atoms from TPMA and the auxiliary ligand coordinated in the fourth site.

When the synthesis of **1** was repeated in methanol, which does not readily coordinate to copper, $[Cu^{I}(TPMA)][BPh_4]$ (**2**) was isolated. Complex **2** was surprisingly found to have a slightly distorted trigonal pyramidal geometry stabilized by a weak cuprophilic interaction at 2.8323(12) Å (Figure 3). The axial $Cu-N_{am}$ bond (2.211(3) Å) was found to be shorter than in the previous examples of copper(I) TPMA complexes (Table 1), and the three equatorial $Cu-N_{py}$ bonds were statistically equivalent with lengths of 2.042(4), 2.037(4), and 2.036(4) Å. In conjunction with the shorter $Cu-N_{am}$ bond length, the copper atom in **2** was displaced to a lesser extent (0.304 Å) from the LSP derived from nitrogen atoms in pyridine rings. The two $[Cu^{I}(TPMA)]^{+}$ cations stabilized by a cuprophilic interaction were arranged in such a way that the pyridyl rings were staggered to achieve minimal steric interference. Weak intermolecular C−H---C interactions were also observed in the crystal lattice ranging from 2.74 to 2.99(6) Å (see Supporting Information).

The salt metathesis of Cu^{I}(TPMA)Br with half equivalent of $NaBPh_4$ formed $[(Cu^{I}(TPMA)_2\text{-}\mu\text{-}Br][BPh_4]$ (**3**) (Figure 4). The formation of **3** was also observed in the synthesis of **2**, unless the byproduct NaBr was rapidly removed from the reaction mixture. Complex **3** exhibited a highly unusual structure where two $[Cu^{I}(TPMA)]^{+}$ cations were bridged by a single bromide anion, creating two pseudo-pentacoordinated moieties each with a distorted tetrahedral geometry. The remaining charge was balanced by a non-coordinating BPh_4^{-} anion. The two sides of the large cation were quite similar, and the pyridyl rings of TPMA were arranged in a pseudo staggered conformation to minimize steric hindrance partially imposed by the Cu1−Br−Cu2 angle (117.46(1)°). The average $Cu1-N_{am}$ bond in **3** was determined to be 2.424(2) Å, which was in good agreement with previously isolated Cu^{I}(TPMA)Cl[2] and Cu^{I}(TPMA)Br[1] complexes. Similarly, the average $Cu1-N_{py}$ bonds ranged from 2.062(2) to 2.112(2) Å. The Cu−Br bond lengths in **3** (2.5228(4) and 2.5564(4) Å) were slightly longer when compared to

(52) Lim, B. S.; Holm, R. H. *Inorg. Chem.* **1988**, *37*, 4898–4908.
(53) Xu, X.; Maresca, K. J.; Das, D.; Zahn, S.; Zubieta, J.; Canary, J. W. *Chem.—Eur. J.* **2002**, *8*, 5679–5683.

Table 1. Structural Comparison of Copper(I) Complexes with TPMA Containing Halide Anions or Monodentate R-C≡N Ligands[a]

complex[b]	Cu−N_{am}	Cu−N_{py}[c]	Cu−N_{AN}	N_{am}−Cu−N_{AN}	Cu−$LSP_{N,py}$[d]	ref.
$[Cu^{I}(L)(AN)][BPh_4]$	2.4109(10)	2.0923(18)	1.9914(11)	175.94(4)	0.545(6)	this work
$[Cu^{I}(L)(AN)][ClO_4]$	2.43(1)	2.09(2)	1.99(1)	179.5(5)	0.545(6)	52
$[Cu^{I}(L')(AN)][PF_6]$	2.439(8)	2.110(11)	1.999(9)	174.9(2)	0.569(6)	14
$Cu^{I}(L)Cl$	2.4366(11)	2.0808(19)			0.534(6)	2, 41
$Cu^{I}(L)Br$	2.4397(14)	2.0825(26)			0.538(6)	1

[a] Bond lengths are given in angstroms (Å) and angles in degrees (deg). [b] L = TPMA, L′ = methyl-6-((bis(2-pyridinylmethyl)amino) methyl)pyridine-3-carboxylate, AN = CH_3CN. [c] Average Cu−N(pyridine) bond length. [d] Distance between copper(I) atom and LSP derived from nitrogen atoms in pyridine rings.

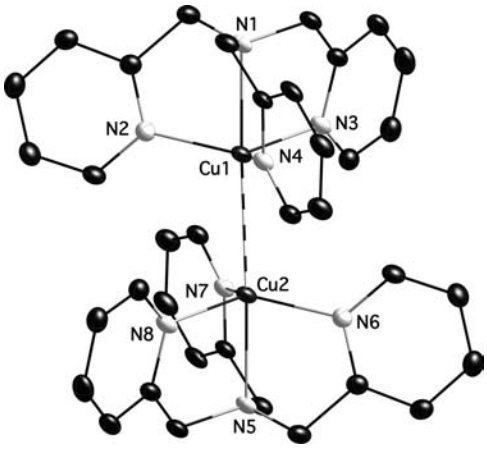

Figure 3. Molecular structure of $[Cu^{I}(TPMA)][BPh_4]$ (**2**) at 150 K, shown with 50% probability displacement ellipsoids. H-atoms and counteranion have been omitted for clarity. Selected distances [Å] and angles [deg]: Cu1−N1 2.211(3), Cu1−N2 2.042(4), Cu1−N3 2.037(4), Cu1−N4 2.036(4), Cu1−Cu2 2.8323(12), N1−Cu1−N2 80.73(13), N1−Cu1−N3 82.08(14), N1−Cu1−N4 81.39(14), N2−Cu1−N3 117.83(15), N2−Cu1−N4 117.49(14), N3−Cu1−N4 118.10(15), Cu1−Cu2−N5 177.73(10), [symmetry codes: (i) $-x+2, -y+2, -z+1$].

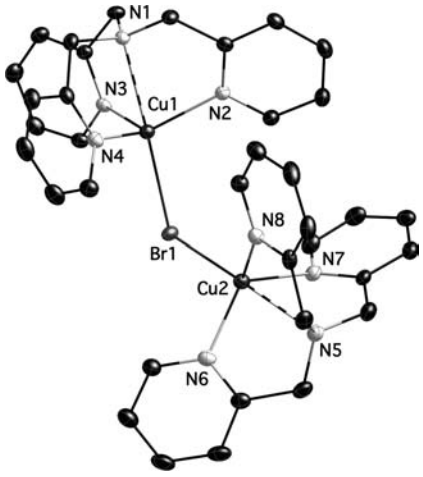

Figure 4. Molecular structure of $[(Cu^{I}(TPMA))_2$-μ-Br$][BPh_4]_2$ (**3**) at 150 K, shown with 50% probability displacement ellipsoids. H-atoms and counteranion have been omitted for clarity. Selected distances [Å] and angles [deg]: Cu1−N1 2.429(2), Cu1−N2 2.067(2), Cu1−N3 2.131(2), Cu1−N4 2.065(2), Cu1−Br1 2.5228(4), N1−Cu1−N2 76.00(7), N1−Cu1−N3 74.08(7), N1−Cu1−N4 75.28(8), N2−Cu1−N3 107.70(8), N4−Cu1−N2 111.32(8), N4−Cu1−N3 121.61(8), Cu1−Br1−Cu2 117.456(13).

$[Cu^{I}(TPMA)Br]$ (2.5088(3) Å), which was presumably a result of the bridging of two Cu^{I} centers. Distorted tetrahedral geometry of Cu1 and Cu2 atoms in $[(Cu^{I}(TPMA)_2$-μ-Br$]^+$ cation was further evident by relatively large displacement from the LSP derived from pyridine nitrogen atoms (0.537(6) and 0.499(6) Å, respectively). Lastly, the crystal structure of **3** was stabilized by a series of weak C−H---C (2.814(6)−2.887(6) Å) and dipole N---H−C (2.643(6) Å) interactions (see Supporting Information).

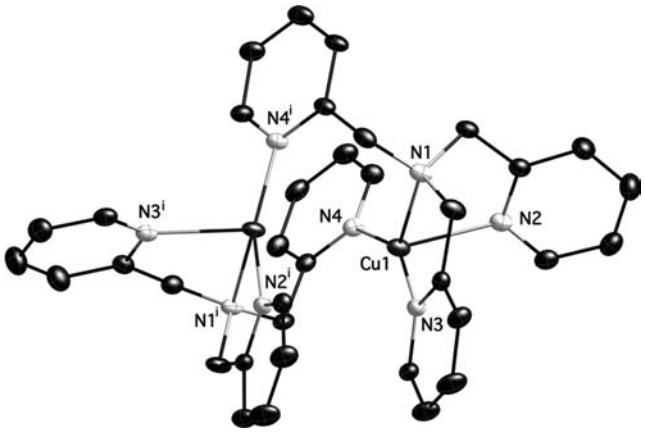

Figure 5. Molecular structure of $[Cu^{I}(TPMA)]_2[ClO_4]_2$*$CH_3OH$ (**4**) at 150 K, shown with 50% probability displacement ellipsoids. H-atoms, counteranions, and solvent molecules have been omitted for clarity. Selected distances [Å] and angles [deg]: Cu1−N1 2.2590(13), Cu1−N2 1.9909(12), Cu1−N3 2.2213(16), Cu1−N4 1.9593(13), N1−Cu1−N2 81.87(5), N1−Cu1−N3 75.63(5), N1−Cu1−N4 123.01(5), N2−Cu1−N3 95.25(5), N2−Cu1−N4 150.49(6), N3−Cu1−N4 105.68(6), [symmetry codes: (i) $-x+1, y, -z+1/2$].

A very different structure was observed when $[Cu^{I}(CH_3CN)_4][ClO_4]$ was reacted with 1 equiv of TPMA in methanol. Instead of a long cuprophilic interaction between two monomeric $[Cu^{I}(TPMA)]^+$ cations, the dimer $[Cu^{I}(TPMA)]_2$-$[ClO_4]_2$*CH_3OH (**4**) was isolated in the solid state. Presumably, copper(I)/TPMA complex rearranged into a dimer via pyridyl arm dissociation and coordination to a second copper(I) center, and vice versa (Figure 5). On the basis of a Cambridge Crystallographic Database search, only one other complex with a structurally similar 6-Ph-TPMA (1-(6-phenylpyridin-2-yl)-*N*,*N*-bis(pyridin-2-ylmethyl)methanamine) ligand and PF_6^- counterion has been reported.[54] Each copper(I) center in **4** was coordinated to four nitrogen atoms with bond lengths of 2.2590(13), 1.9909(12), 2.2213(16), and 1.9593(13) Å, respectively. The bond angles between the copper(I) center and N2, N3, and N4 atoms (75.63(5)°, 81.87(5)°, and 95.25(5)°, respectively) indicated distortions from ideal tetrahedral geometry. Furthermore, the larger angles in this complex were associated with the bridging pyridine N4 atom (N3−Cu1−N4 105.68(6)°, N1−Cu1−N4 123.01(5)°, and N2−Cu1−N4

(54) Jensen, M. P.; Que, E. L.; Shan, X.; Rybak-Akimova, E.; Que, L. J. *J. Chem. Soc., Dalton Trans.* **2006**, *29*, 3523–3527.

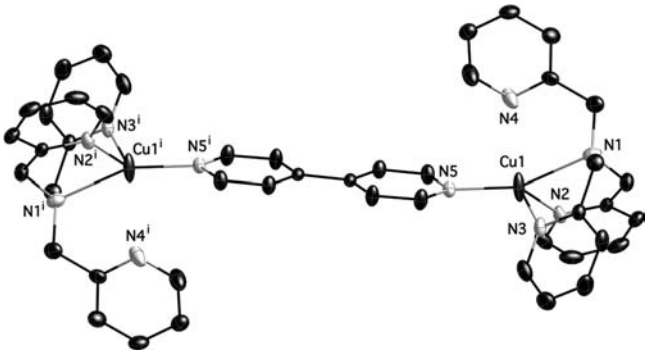

Figure 6. Molecular structure of $[(Cu^{I}(TPMA))_2(4,4'\text{-dipy})][BPh_4]_2$ (**5**) at 150 K, shown with 50% probability displacement ellipsoids. H-atoms and counteranions have been omitted for clarity. Selected distances [Å] and angles [deg]: Cu1−N1 2.325(3), Cu1−N2 2.052(3), Cu1−N3 2.085(2), Cu1---N4 2.523(6), Cu1−N5 1.998(2), N1−Cu1−N2 78.59(9), N1−Cu1−N3 77.53(9), N1−Cu1−N5 157.08(9), N2−Cu1−N3 102.06(9), N2−Cu1−N5 118.82(9), N3−Cu1−N5 110.33(9), [symmetry codes: (i) $-x+1, -y+2, -z$, (ii) $-x+1, -y+1, -z$].

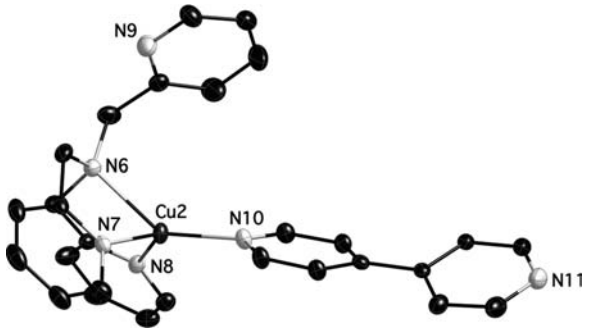

Figure 7. Molecular structure of $[Cu^{I}(TPMA)(4,4'\text{-dipy})][BPh_4]$ (**6**) at 150 K, shown with 50% probability displacement ellipsoids. H-atoms and counteranions have been omitted for clarity. Selected distances [Å] and angles [deg]: Cu2−N6 2.248(2), Cu2−N7 2.065(2), Cu2−N8 2.043(2), Cu2−N10 1.970(2), N6−Cu2−N7 78.60(9), N6−Cu2−N8 80.75(9), N6−Cu2−N10 141.14(9), N7−Cu2−N8 116.98(9), N7−Cu2−N10 118.09(9), N8−Cu2−N10 115.09(9).

150.49(6)°). The molecular structure of $[Cu^{I}(TPMA)]_2[ClO_4]_2{*}CH_3OH$ was stabilized by weak C−H---C contacts between TPMA ligands with distances ranging from 2.806(6) to 2.994(6) Å. Additionally, weak Cl−O---H−C and Cl−O---H−O interactions were detected between the ClO_4^- counterion and TPMA ligand (2.562(6)−2.627(6) Å), and ClO_4^- and CH_3OH solvate (2.403(6)−2.678(6) Å) (see Supporting Information).

While changing the anion in copper(I) complexes with TPMA ligand has produced a wide variety of molecular structures with different degrees of steric hindrance around the copper(I) center, preliminary studies have indicated that such variations had small effect on the reaction rate in ATRA containing free radical diazo initiators as reducing agents. Recent kinetic studies of this process revealed that the rate of alkene consumption was dependent on the concentration and rate of decomposition of the radical initiator, but independent of the concentration of the copper catalyst.[23,32,55] Therefore, more precise kinetic data could be provided by careful measurements of the activation (Cu^{I} + RX → $Cu^{II}X$ + R$^{\bullet}$) and deactivation ($Cu^{II}X$ + R$^{\bullet}$ → Cu^{I} + RX) rate constants, which are currently being conducted in our laboratories. If the activation in ATRA catalyzed by copper(I)/TPMA complexes is proceeding via an inner sphere electron transfer and does not increase in the presence of non-coordinating anions, then it is possible that arm dissociation from TPMA could create an open coordination site necessary for the homolytic cleavage of the carbon-halide bond. By coordinating ligands of different steric bulk to $[Cu^{I}(TPMA)][BPh_4]$ (**2**), this possibility could be structurally examined. The bidentate bridging ligand 4,4′-dipyridyl (4,4′-dipy) was added to complex **2** as a slightly larger alternative to acetonitrile. Several equivalents of the ligand were used to obtain X-ray quality crystals, and two complexes were identified in the unit cell, the bridged $[(Cu^{I}(TPMA)_2(4,4'\text{-dipy})][BPh_4]$ (**5**) (Figure 6) and $[Cu^{I}(TPMA)(4,4'\text{-dipy})][BPh_4]$ (**6**) (Figure 7). The coordination of 4,4′-dipyridyl sterically forced dissociation of one arm of TPMA ligand in both cases, resulting in a distorted tetrahedral geometry. The N_{am}−Cu1−$N_{4,4'\text{-dipy}}$ bond angle was more skewed in complex **6** (141.14(9)°) which resulted in displacement of N9 pyridyl nitrogen atom further away from copper(I) center (Cu1−N9 = 4.360(6) Å), in contrast to complex **5** (157.08(9)°) where the ousted nitrogen atom appeared to be weakly interacting with copper (Cu1−N4 = 2.523(6) Å). In addition, the alkyl amine-copper bond was also shorter in **6** (Cu2−N6 = 2.248(2) Å) than in **5** (Cu1−N1 = 2.325(3) Å). In both complexes, the remaining copper-pyridyl nitrogen bonds from TPMA ligand were relatively unchanged (2.052(3) and 2.085(2) Å for **5**; 2.065(2) and 2.043(2) Å for **6**), and the distance to 4,4′-dipyridyl was also similar (1.998(2) and 1.970(2) Å, respectively). Furthermore, coordinated 4,4′-dipyridyl was found to be planar in complex **5**, and slightly twisted in **6** with a torsion angle of 24.76(6)°. The free 4,4′-dipyridyl molecule found in the structure served to stabilize the crystal packing via weak N---H−C dipole interactions at 2.707(6) Å (see Supporting Information). Additionally, the non-coordinating N11 in **6** was found to weakly interact with the copper atom of adjacent molecule at the distance of 3.438(6) Å, which could explain the non-planarity of 4,4′-dipyridyl discussed above. It is also interesting to note that both **5** and **6** appear to be much more air stable than the corresponding copper(I) complexes with halide anions and/or acetonitrile.

To study the outcome of larger monodentate ligand complexation to $[Cu^{I}(TPMA)][BPh_4]$, triphenylphosphine (PPh_3) was used to synthesize $[Cu^{I}(TPMA)(PPh_3)][BPh_4]$ (**7**). The coordination of PPh_3 had even larger effect on arm dissociation of TPMA ligand than 4,4′-dipyridyl, displacing the N4 pyridyl atom by 3.258(6) Å (Figure 8). As a result, complex **7** was distorted tetrahedral in geometry, and the complexation to copper(I) center occurred through the aliphatic (Cu1−N1 = 2.2089(14) Å) and two pyridine (Cu1−N2 = 2.0661(14) Å and Cu1−N3 = 2.1083(15) Å) nitrogen atoms of TPMA, and phosphorus atom from PPh_3 (Cu1−P1 = 2.1852(5) Å). The structural features of **7** were similar to $[Cu^{I}(TPMA)(PPh_3)][PF_6]$, with the exception that in the latter complex the nitrogen atom from the displaced arm in TPMA was pointing away from copper (Cu−N = 6.530(2) Å).[14] This could be attributed to a much smaller N1−Cu1−P1 bond angle (127.8°) when compared to **7** (141.78(4)°). Nevertheless, the Cu−N4 bond distance in **7** (3.258(6) Å) was longer than the sum of van der Waals radii (2.95 Å), indicating negligible interactions between the displaced pyridyl

(55) Balili, M. N. C.; Pintauer, T. *Polym. Prepr.* (*Am. Chem. Soc., Div. Polym. Chem.*) **2008**, *49*(2), 161–162.

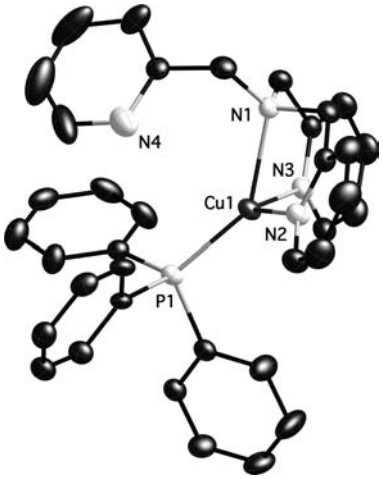

Figure 8. Molecular structure of $[Cu^{I}(TPMA)PPh_3][BPh_4]$ (**7**) at 150 K, shown with 50% probability displacement ellipsoids. H-atoms and counteranions have been omitted for clarity. Selected distances [Å] and angles [deg]: Cu1−N1 2.2089(14), Cu1−N2 2.0661(14), Cu1−N3 2.1083(15), Cu1−P1 2.1852(5), N1−Cu1−N2 81.08(5), N1−Cu1−N3 78.86(5), N2−Cu1−N3 117.66(6), N1−Cu1−P1 141.78(4), P1−Cu1−N2 119.17(4), P1−Cu1−N3 112.65(4).

Table 2. Structural Comparison of Complexes **1**, **5**, **6**, and **7** with the General Formula $[Cu^{I}(TPMA)(L)][BPh_4]$ (L = CH_3CN, 4,4′-dipyridyl, or PPh_3)[a]

complex	**1**	**5**	**6**	**7**
L_{aux}	CH_3CN	4,4-dipy	4,4′-dipy	PPh_3
$Cu-N_{am}$	2.4109(10)	2.325(3)	2.248(2)	2.2089(14)
$Cu-N_{py,1}$	2.1031(10)	2.052(3)	2.065(2)	2.0661(14)
$Cu-N_{py,2}$	2.1114(11)	2.085(2)	2.053(2)	2.1083(15)
$Cu-N_{py,3}$	2.0624(10)	2.523(6)	4.360(5)	3.258(6)
$Cu-L_{aux}$	1.9914(11)	1.998(2)	1.970(2)	2.1852(5)
$N_{am}-Cu-L_{aux}$	175.94(4)	157.08(9)	141.14(9)	141.78(4)
$Cu-Py_{centroid}$[c]	3.481	3.824	4.305	4.217
cone angle[b]	37.8	86.5	87.4	141.72

[a] Selected bond lengths are given in angstroms (Å) and the cone angles in degrees (deg). [b] Cone angle was calculated for the auxiliary ligand using Mercury 3.2 software. [c] Distance between the copper(I) atom and centroid point derived from nitrogen and carbon atoms in the pyridine ring furthest away from copper.

nitrogen atom and copper. Intermolecular interactions observed in the unit cell included only weak C−H- - -C contacts ranging from 2.809 to 2.850(6) Å (see Supporting Information).

The auxiliary ligands used in the above-discussed complexes (acetonitrile, 4,4′-dipyridyl, and triphenylphosphine) are all strong σ-donors, but vary drastically in terms of steric bulk. Therefore, these monodentate ligands should have different effects on TPMA coordination in copper(I) complexes. To quantitatively assess the steric bulk of each ligand, cone angles[56] were calculated from the molecular structures using a previously reported method.[57] As indicated in Table 2, acetonitrile in complex **1** was found to have a cone angle of 37.80°, which did not result in arm dissociation of TPMA ligand. However, the larger 4,4′dipyridyl, with a cone angle of 86.46° in **5** and 87.26° in **6**, displaced one of the pyridine rings in TPMA by 3.824 and 4.305 Å, respectively (the distance was calculated between the copper(I) atom and centroid point derived from nitrogen and carbon atoms in the pyridine ring). The effect was also observed for triphenylphosphine

(56) Tolman, C. A. *Chem. Rev.* **1977**, *77*, 313–348.
(57) Muller, T.; Mingos, M. P. *Trans. Met. Chem.* **1995**, *20*, 533–539.

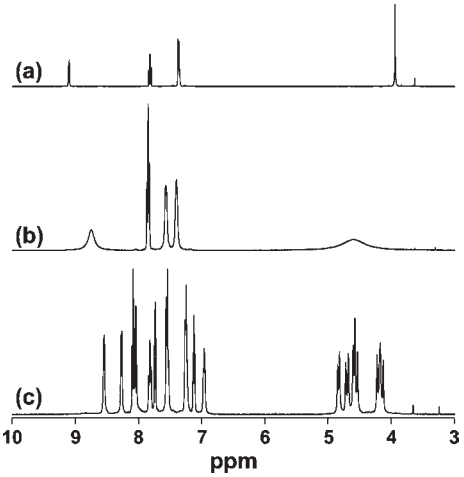

Figure 9. ^1H NMR spectra (400 MHz, $(CD_3)_2CO$) of $[Cu^{I}(TPMA)Br]$ at 180 K (a), $[Cu^{I}(TPMA)][ClO_4]$ at 298 K (b), and $[Cu^{I}(TPMA)]_2[ClO_4]_2$ at 185 K (c).

(cone angle = 141.72°) in complex **7**, in which the same distance was determined to be 4.217 Å. Although there appears to be no direct correlation between the cone angle and pyridine ring displacement from the copper(I) center, it is apparent that the latter does to some extend depend on the steric bulk of the auxiliary ligand. Studies on the effect of these monodentate ligands on catalytic activity in ATRA are currently underway in our laboratories.

Solution Studies of Copper(I) Complexes. Variable temperature ^1H NMR spectroscopy was used to probe structures of copper(I) complexes with TPMA ligand in solution. This technique was previously shown to be useful in examining the structure of $Cu^{I}(TPMA)Br$,[1] which was found to be highly symmetrical and monomeric in solution, as indicated by chemically equivalent pyridine rings (Figure 9A). A very similar ^1H NMR spectrum was also observed for $[Cu^{I}(TPMA)(CH_3CN)][BPh_4]$ (**1**) (see Supporting Information). In **1**, a singlet for acetonitrile was shifted downfield by approximately 1.6 ppm in acetone-d_6 upon cooling from 298 to 180 K, indicating a deshielding effect as a result of coordination. On the other hand, $[Cu^{I}(TPMA)]_2[ClO_4]*CH_3OH$ (**4**), exhibited four broad resonances at room temperature similar to $Cu^{I}(TPMA)Br$, suggesting the structure was also monomeric (Figure 9B). Interestingly, upon cooling to 185 K, evidence for dimer formation consistent with the solid state structure was clearly observed by the emergence of three sets of unequal peaks between 8.54 and 6.95 ppm for the pyridyl and 4.82 and 4.17 ppm for the methylene protons (Figure 9C). When the same complex was dissolved in acetonitrile-d_3, only peaks corresponding to the monomer were observed, indicating the formation of $[Cu^{I}(TPMA)(CD_3CN)][ClO_4]$. Similarly, at room temperature $[Cu^{I}(TPMA)][BPh_4]$ (**2**) also exhibited a monomeric structure resembling **1**. However, upon cooling to 180 K, the peaks associated with the dimer formation clearly emerged in relatively equal proportions relative to the monomer. Therefore, it is likely that an equilibrium between the monomer and dimer exists in solution for complex **2** as shown in Scheme 3.

The ^1H NMR spectrum for $[(Cu^{I}(TPMA)_2\text{-}\mu\text{-}Br][BPh_4]$ (**3**) showed five peaks for TPMA at 9.17, 7.78, 7.40, 7.08, and 4.03 ppm (see Supporting Information). This suggested that the complex had highly symmetrical structure in solution, which was inconsistent with the solid state in

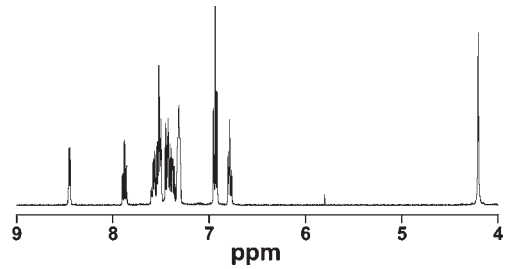

Figure 10. ^{1}H NMR (400 MHz, 180 K, $(CD_3)_2CO$) spectrum of $[Cu^I(TPMA)PPh_3][BPh_4]$.

Scheme 3. Proposed Equilibrium between Monomeric $[Cu^I(TPMA)][BPh_4]$ and Dimeric $[Cu^I(TPMA)]_2[BPh_4]_2$ in the Absence of a Coordinating Solvent

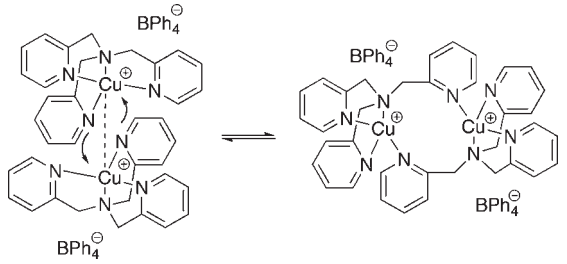

which two $[Cu^I(TPMA)]^+$ cations were bridged by bromide anion at an angle of 117.46(1)°. We ruled out the possibility for dissociation because it would have resulted in the formation of $Cu^I(TPMA)Br$, $[Cu^I(TPMA)][BPh_4]$, and $[Cu^I(TPMA)]_2[BPh_4]_2$, which was not observed experimentally using low temperature ^{1}H NMR studies. Similarly to **1** and **3**, $[Cu^I(TPMA)(PPh_3)][BPh_4]$ (**7**) also showed five resonances for TPMA ligand, indicating that in solution all three pyridyl arms were symmetrically coordinated to the copper(I) center (Figure 10). However, the chemical shift of the proton in closest proximity to the pyridyl nitrogen showed a significant upfield shift (8.46 ppm), in contrast to **1** (8.65 ppm) or $Cu^I(TPMA)Br$ (9.10 ppm), which was presumably the result of σ-donation from the coordinated triphenylphosphine. This was also confirmed by $^{31}P\{^1H\}$ NMR which showed a downfield shift of 8.9 ppm relative to free phosphine.

Solid-State Structural Studies of Copper(II) Complexes. ATRA is commonly performed starting with the copper(II) complex or deactivator because of its oxidative stability. When such complex is reduced in the presence of radicals generated by the decomposition of initiator such as AIBN, the copper(I) or activator is formed which starts the catalytic cycle by homolytically cleaving an alkyl halide bond. To investigate the counterion effect on the structure of copper(II) complexes with TPMA ligand $[Cu^{II}(TPMA)Cl][ClO_4]$ (**8**), $[Cu^{II}(TPMA)Cl][BPh_4]$ (**9**), $[Cu^{II}(TPMA)Br][ClO_4]$ (**10**), and $[Cu^{II}(TPMA)Br][BPh_4]$ (**11**) where synthesized by salt methathesis of previously reported $[Cu^{II}(TPMA)X][X]$ ($X = Br^-$ or Cl^-) complexes.[1,2] Although **8** and **9** were crystallographically quite different from $[Cu^{II}(TPMA)Cl][Cl]$, $[Cu^{II}(TPMA)Cl]^+$ cations were nearly identical in both cases (Table 3). Each copper(II) cation in **8** and **9** was distorted trigonal bipyramidal in geometry, as a result of coordination of four nitrogen atoms from TPMA ligand and one chlorine atom. (Figure 11). The $Cu^{II}-Cl$ bonds in **8** (2.2390(5) Å) and **9** (2.2341(3) Å) were very similar to the corresponding chloride complex (2.2369(4) Å). Furthermore, the copper(II) atom in complexes **8** and **9** was displaced from the LSP derived from nitrogen atoms in pyridine rings by 0.317(6) (averaged) and 0.299(6) Å respectively, which also compared well with $[Cu^{II}(TPMA)Cl][Cl]$ (0.335(6) Å). Complexes **8** and **9** lacked perfect crystallographic 3-fold symmetry with respect to Cu−Cl or $Cu-N_{am}$ vector observed in $[Cu^{II}(TPMA)Cl][Cl]$, which was presumably due to the presence of more bulky ClO_4^- and BPh_4^- counterions. However, the cations in each case had nearly perfect (non-crystallographic) C_3 symmetry. The intermolecular interactions in **8** consisted mostly of O---H−C dipole interactions between the perchlorate counterion and TPMA ligand, which ranged from 2.396(6) to 2.694(6) Å. Weak Cl---H−C attractions between the coordinated chloride and TPMA ligand in the adjacent molecule were also observed ranging from 2.793(6) to 2.860(6) Å (see Supporting Information). On the other hand, the crystal structure of complex **9** was stabilized by weak C−H---C contacts involving the anion, TPMA, and a solvent acetonitrile with distances ranging from 2.669(6) to 2.884(6) Å. Lastly, two Cl---H−C interactions were also detected between the chlorine atom and TPMA with distances of 2.857(6) and 2.840(6) Å, respectively (see Supporting Information).

The corresponding bromide complexes, $[Cu^{II}(TPMA)Br][ClO_4]$ (**10**) and $[Cu^{II}(TPMA)Br][BPh_4]$ (**11**), were found to be structurally similar to the chlorides **8**, **9**, and

Table 3. Structural Comparison of $[Cu^{II}(TPMA)Cl][A]$ ($A = Cl^-$, ClO_4^- (**8**) and BPh_4^- (**9**)) Complexes[a]

parameter	$[Cu^{II}(TPMA)Cl][Cl]$[b]	**8**[c]	**9**[c]
$Cu1-N1_{ax}$	2.0481(14)	2.0413(15)	2.0555(8)
$Cu1-N2_{eq}$	2.0759(8)	2.1115(16)	2.0304(10)
$Cu1-N3_{eq}$	2.0759(8)	2.0567(16)	2.0876(9)
$Cu1-N4_{eq}$	2.0759(8)	2.0292(16)	2.0505(9)
$Cu1-N_{eq,av.}$[d]	2.0759(8)	2.0658(28)	2.0562(18)
Cu1−Cl1	2.2369(4)	2.2390(5)	2.2341(3)
N1−Cu1−N2	80.71(2)	81.05(7)	81.60(4)
N1−Cu1−N3	80.71(2)	80.63(6)	80.83(4)
N1−Cu1−N4	80.71(2)	81.97(6)	82.36(3)
N2−Cu1−N3	117.447(12)	108.44(6)	115.65(4)
N3−Cu1−N4	117.447(12)	126.20(6)	110.49(4)
N4−Cu1−N2	117.447(12)	118.43(6)	127.52(4)
Cl1−Cu1−N2	99.29(2)	99.23(5)	98.49(3)
Cl1−Cu1−N3	99.29(2)	99.88(5)	99.47(3)
Cl1−Cu1−N4	99.29(2)	97.33(5)	97.28(3)
Cl1−Cu1−N1	180.000(19)	179.29(5)	179.60(3)

[a] Bond lengths are given in angstroms (Å) and angles in degrees (deg). [b] ref 2. [c] This work, values for complex **8** are averaged from two molecules in the asymmetric unit. [d] Average Cu−N equatorial bond length.

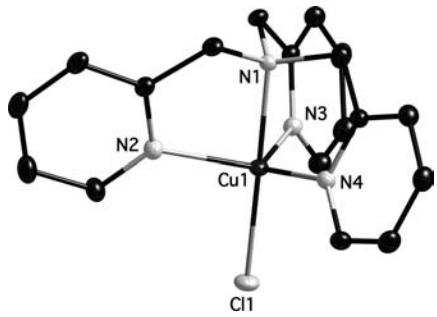

Figure 11. Molecular structure of $[Cu^{II}(TPMA)Cl][ClO_4]$ (**8**) at 150 K, shown with 50% probability displacement ellipsoids. H-atoms and counteranion have been omitted for clarity.

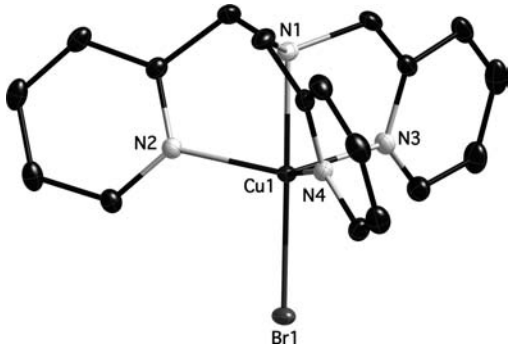

Figure 12. Molecular structure of $[Cu^{II}(TPMA)Br][ClO_4]$ (**10**) at 150 K, shown with 50% probability displacement ellipsoids. H-atoms and counteranion have been omitted for clarity.

Table 4. Selected Bond Lengths [Å] and Angles [deg] for $[Cu^{II}(TPMA)Br][A]$ (A = Br^-, ClO_4^- (**10**) and BPh_4^- (**11**)) Complexes

parameter	$[Cu^{II}(TPMA)Br][Br]^a$	**10**^{b}	**11**^{b}
Cu1−N1$_{ax}$	2.040(3)	2.0387(17)	2.0534(11)
Cu1−N2$_{eq}$	2.073(2)	2.0642(18)	2.0545(12)
Cu1−N3$_{eq}$	2.073(2)	2.0515(17)	2.0328(12)
Cu1−N4$_{eq}$	2.073(2)	2.1163(18)	2.0909(12)
Cu1−N$_{eq,av.}$^{c}	2.073(2)	2.0773(31)	2.0594(21)
Cu1−Br1	2.3836(6)	2.3765(3)	2.3711(2)
N1−Cu1−N2	80.86(5)	80.36 (7)	82.32(5)
N1−Cu1−N3	80.86(5)	81.44(7)	81.55(5)
N1−Cu1−N4	80.86(5)	81.03(7)	80.98(5)
N2−Cu1−N3	117.53(3)	124.95(7)	128.21(5)
N3−Cu1−N4	117.53(3)	117.89(7)	115.28(5)
N4−Cu1−N2	117.53(3)	109.80(7)	110.17(5)
Br1−Cu1−N2	99.14(5)	100.44(5)	97.55(3)
Br1−Cu1−N3	99.14(5)	97.76(5)	98.68(3)
Br1−Cu1−N4	99.14(5)	99.03(5)	98.89(4)
Br1−Cu1−N1	180.00(5)	179.11(5)	179.77(3)

^{a} ref 1. ^{b} This work, values for complex **10** are averaged for two molecules in the asymmetric unit. ^{c} Average Cu−N equatorial bond length.

$[Cu^{II}(TPMA)Cl][Cl]$ discussed above (Figure 12). The cations lacked perfect crystallographic 3-fold symmetry observed in $[Cu^{II}(TPMA)Br][Br]$,[1] but pyridine rings in coordinated TPMA ligand were nearly symmetrical with respect to C_3 rotation. From the point of view of TPMA coordination, these complexes were also comparable to previously discussed **8** and **9**. While the typical Cu^{II}−Cl bond length in **8** and **9** was close to 2.23 Å, the Cu^{II}−Br bond distance in **10** and **11** was found to be longer as a result of the larger atomic radii of bromine atom (2.3765(3) and 2.3711(2) Å, respectively). The copper(II) atom was displaced from the LSP by 0.330(6) (averaged) in complex **10** and 0.299(6) Å in **11**, which compared well with the bromide complex (0.329(6) Å) (Table 4). No other significant differences in the structures were observed.

Additionally, intermolecular interactions in **10** and **11** were found to closely resemble **8** and **9**. The crystal structure of **10** was stabilized by predominately strong C−H---O dipole forces at distances ranging from 2.429(6) to 2.620(6) Å, and two weaker C−H---Br dipole contacts (2.963(6)−2.987(6)) Å. Furthermore, one van der Waals C−H---C interaction between coordinated TPMA ligands was found to exist at 2.875(6) Å (see Supporting Information). In the crystal structure of **11**, weak C−H---C contacts ranging from 2.703(6) to 2.892(6) Å, as well as weak C−H---Br dipole interactions at 2.951(6) and 2.921(6) were observed Å (see Supporting Information).

In solution, **8**, **9**, **10**, and **11** were found to have similar UV−vis spectra ($\lambda_{max} \approx 960$ nm, $\varepsilon_{max} \approx 190$ L mol^{-1} cm^{-1}), indicating negligible interactions of anions with the copper(II) centers, consistent with the solid state studies discussed above.

Conclusions

In conclusion, the effects of counterions (Cl^-, Br^-, ClO_4^-, and BPh_4^-) and auxiliary ligands (Cl^-, Br^-, CH_3CN, 4,4′-dipyridyl, and PPh_3) on the structures of copper(I) and copper(II) complexes with TPMA ligand were investigated. Copper(I)/TPMA complexes with Br^- and CH_3CN were found to be distorted tetrahedral in geometry, and each copper(I) center was coordinated by an auxiliary monodentate ligand and three nitrogen atoms from pyridyl rings. In these complexes, the axial elongation of Cu^I−N_{am} bond (~2.4 Å) was observed, indicating not only the rigidity of TPMA ligand, but also the strong preference for copper(I) to adopt four coordinated geometry. In the absence of monodentate ligand, two structures were observed. A monomeric trigonal pyramidal $[Cu^I(TPMA)][BPh_4]$ complex was characterized in the solid state, which was stabilized by a weak cuprophilic interaction (2.8323(12) Å). On the other hand, $[Cu^I(TPMA)]_2[ClO_4]_2$ was found to be dimeric in which dissociated pyridyl arms of TPMA ligand bridged two copper(I) centers. In copper(I) complexes containing larger auxiliary ligands such as 4,4′-dipyridyl or PPh_3, a pyridyl arm of TPMA ligand was found to partially or totally dissociate. These complexes were all monomeric in the solid state, with the exception of $[(Cu^I(TPMA))_2(4,4'\text{-dipy})][BPh_4]_2$ in which 4,4′-dipyridyl ligand bridged two $[Cu^I(TPMA)]^+$ cations.

Copper(II) complexes with the general formula $[Cu^{II}(TPMA)X][Y]$ (X = Cl^-, Br^- and Y = ClO_4^-, BPh_4^-) were synthesized and characterized in the solid state to investigate the counterion effect on the structure of $[Cu^{II}(TPMA)X]^+$. In each complex, the copper(II) atom was found to be distorted trigonal bipyramidal in geometry with nearly perfect C_3 symmetry for coordinated TPMA ligand. The average Cu^{II}−N bond distances were found to range between 2.03 and 2.12 Å, consistent with previous studies.

Acknowledgment. Financial support from National Science Foundation Career Award (CHE-0844131) is gratefully acknowledged

Supporting Information Available: Crystal tables, ^{1}H NMR spectra, infrared spectra, full crystal structures, and crystal packing diagrams. This material is available free of charge via the Internet at http://pubs.acs.org.